Journal of Bioenergetics and Biomembranes, Vol. 21, No. 4, 1989

MINI-REVIEW

Structure of the Mitochondrial Outer Membrane Channel Derived from Electron Microscopy of 2D Crystals

Carmen A. Mannella[1,2]

Received May 25, 1989

Abstract

A structural model for the channel in the mitochondrial outer membrane is presented, derived from electron microscopic studies of two-dimensional crystals and inferences from the primary structure of the 30-kDa polypeptide which forms the channel. The channel is represented as a cylindrical beta-barrel, with a carbon backbone diameter of 3.8 nm. The axial projection of the cylinder is divided radially into four sectors by four interchannel contact points. These sectors are characterized in terms of their interactions with lipid and macromolecular ligands, and in terms of the presence or absence of exposed basic amino acids.

Key Words: Mitochondrial outer membrane; channel; electron microscopy; image processing.

Background

The most remarkable property of the mitochondrial outer membrane is its extreme permeability to metabolites and ions. That this distinctive characteristic is due to large, passive diffusion channels in the membrane comes from several lines of investigation. Numerous channel-like subunits were first detected in electron micrographs of negatively stained plant mitochondrial outer membranes in the mid-1960's (Parsons *et al.*, 1965). The presence of

[1]Wadsworth Center for Laboratories and Research, New York State Department of Health, Empire State Plaza, P.O. Box 509, Albany, New York 12201-0509.
[2]Department of Biomedical Sciences, School of Public Health, State University of New York at Albany, Albany, New York 12222.

0145-479X/89/0800-0427$06.00/0

prominent in-plane components in the plant membrane was later confirmed by X-ray scattering experiments and shown to correlate with a major trypsin-resistant 30-kDa polypeptide (Mannella and Bonner, 1975). Shortly thereafter, bilayer reconstitution studies indicated the existence of a potent pore-forming component in mitochondria (Schein *et al.*, 1976). This component was localized to the mitochondrial outer membrane by Colombini (1979) and later identified with the prominent 30-kDa polypeptide by him and others (Zalman *et al.*, 1980; Freitag *et al.*, 1982; Linden *et al.*, 1982; Roos *et al.*, 1982; Colombini, 1983).

The mitochondrial outer membrane channel has been named VDAC, for voltage-dependent, anion-selective channel (Schein *et al.*, 1976). The channel protein has also been referred to as mitochondrial porin, by analogy with the pore-forming polypeptides in outer envelopes of gram-negative bacteria. Whether or not VDAC and the porins are evolutionarily related is unclear. Comparisons of available VDAC and porin sequences have turned up no significant homology (Mannella and Auger, 1986; Forte *et al.*, 1987; Kleene *et al.*, 1987). However, a region of moderate similarity has been found near the C-termini of yeast VDAC and *Neurospora* mitochondrial adenine nucleotide carrier (31% amino acid identity over a stretch of 57 residues) (Mannella and Auger, 1986). This observation and subsequent comparisons involving the *Neurospora* VDAC sequence (Kleene *et al.*, 1987) raise the possibility that the mitochondrial outer membrane pore protein may be related to the family of inner membrane transport proteins described by Aquila *et al.* (1987).

As its name implies, VDAC has two noteworthy functional characteristics: it switches to lower-conductance substates when small transmembrane potentials are applied and, despite its large size (step conductance = 4.3 nS in 1 M KCl), it is more permeable to anions than to cations. The relative ease with which VDAC can be functionally reconstituted, the recent advances in genetic manipulation of the polypeptide (Blachly-Dyson *et al.*, 1989), and the availability of the channel in planar crystalline form (see below) make VDAC a useful model for studying structure–function relationships in a voltage-gated, ion-selective channel.

Electron Microscopy and Image Analysis

Most of the available structural information about the channel in the mitochondrial outer membrane has come from studies using electron microscopy and computer image processing. These studies have been greatly facilitated by the tendency of the channels in the *Neurospora* membrane to form extended two-dimensional periodic arrays. Quasi-optical Fourier

filtration (which takes advantage of the segregation of periodic and random image components in Fourier space) and correlation averaging (which corrects for lattice disorder) have been used to obtain average projections from low-dose images of the arrays in a variety of experimental conditions. [The experimental techniques are described in detail in Mannella *et al.* (1986).] Early research primarily utilized specimens embedded in negative stains, such as uranyl and phosphotungstate salts. More recently, aurothioglucose embedding has been employed to avoid positive staining effects obtained with complex ion solutions. Systematic cryo-electron microscopic studies of vitreous ice-embedded specimens are now underway which are providing direct structural information about the channel in the absence of stains.

Channel Crystallization

Crystallization of VDAC channels is induced *in vitro* by treatment of isolated mitochondrial outer membranes with soluble phospholipase A_2 (Mannella, 1984). Similar periodic channel arrays are sometimes seen in untreated membranes (Mannella, 1982) and have been attributed to the presence of endogenous phospholipase A_2 activity in mitochondrial fractions (Mannella, 1988). Since the endogenous phospholipase is Ca-activated, it has been suggested that crystallization of the VDAC channels may be triggered *in vivo* by elevated cytosolic (or intramitochondrial) Ca^{2+} levels (Mannella, 1988). [Aggregation of the channels may alter their functional characteristics, as in the case of acetylcholine receptor; see Young and Poo (1983).]

The periodic arrays produced from native mitochondrial outer membranes typically contain 600–800 unit cells, each holding six channels. Recently, it has been shown that prefusion of the membranes leads to formation of coherent two-dimensional crystals containing several thousand unit cells (Mannella, 1989). These larger VDAC crystals are useful for high-resolution imaging experiments in the absence of stain.

The crystalline VDAC arrays observed in mitochondrial outer membrane fractions are polymorphic (Mannella *et al.*, 1983, 1986; Mannella, 1985). The most common form is a parallelogram array with lattice dimensions $a = 13$ nm, $b = 11.5$ nm, and a lattice angle of 109° (Fig. 1A). The unit cell contains six sites of dense stain accumulation (the channel lumens), arranged in a hexameric group with two-fold rotational symmetry. The rows in the array can slide with respect to each other (in the horizontal direction in Fig. 1A), causing an overall contraction of the lattice. However, the arrangement of channels within the rows is invariant in the normal and contracted arrays. A third array type is also observed with apparent *p2mg*

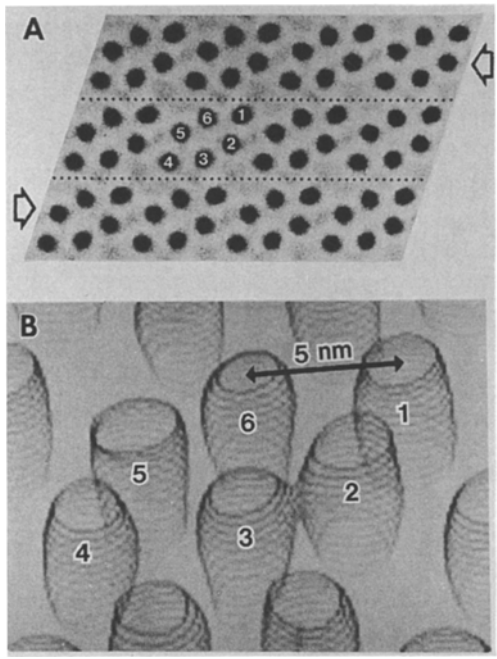

Fig. 1. (A) Fourier-averaged electron microscopic image of *Neurospora* VDAC array, negatively stained with phosphotungstate. This is an example of the oblique array, lattice angle = 109°. The directions in which the horizontal rows slide (see text) are indicated by arrows. (B) Three-dimensional view of the stain-filled cylindrical channels (contours) in the plane of the mitochondrial outer membrane.

symmetry, containing only two channels per unit cell. The possible relationship of this array to the others has been described elsewhere (Mannella *et al.*, 1983; Mannella, 1985).

Size of the VDAC Channel

The center-to-center spacings between adjacent channels in crystalline *Neurospora* VDAC arrays fall in the range 4.3–5.3 nm. This agrees well with a subunit diameter of 4.5–5 nm inferred from radial Patterson function analysis of X-ray scattering data from plant mitochondrial outer membranes (Mannella and Bonner, 1975).

The three-dimensional structure of VDAC arrays embedded in negative stain has been reconstructed from electron microscopic projections of tilted specimens (Mannella *et al.*, 1984). The channel lumens in the oblique array are seen as stain-filled cylinders normal to the membrane plane (Fig. 1B).

The mean diameter of the channel lumen has been inferred from the projected diameters of these cylinders. In uranyl salts and aurothioglucose, the mean inner diameter is 2.5 nm. A somewhat larger diameter obtained with phosphotungstate (3–3.5 nm) has been attributed to positive staining of basic amino acids by the anionic stain (see below) (Mannella and Frank, 1984, 1986; Mannella *et al.*, 1986).

Average images of unstained, oblique arrays of frozen-hydrated crystalline VDAC have recently been obtained (Mannella and Cognon, 1989; Mannella *et al.*, 1989). These maps of the projected density of crystalline VDAC have been compared with projections of thin-walled, hollow cylinders aligned perpendicular to the lattice plane. Close agreement has been found between data and model within a very narrow range of cylinder diameters: 3.8 ± 0.1 nm. (Note that this diameter is measured from the centers of the walls of the cylinders.)

The sequence of yeast VDAC has a marked pattern of alternating polar/nonpolar residues (Mihara and Sato, 1985; Forte *et al.*, 1987). Such a pattern (also present in the *Neurospora* sequence; see Kleene *et al.*, 1987) lends itself neatly to an antiparallel beta-sheet structure for the channel, in which successive residues point into the channel lumen (polar) and out toward the lipid (nonpolar) (Forte *et al.*, 1987). If the hollow cylinder inferred from the frozen-hydrated projection data is equated with the beta-barrel suggested by the sequence, then the carbon backbone of the barrel would have a diameter of 3.8 nm. Assuming a layer of amino acid residues to extend about 0.5 nm from either side of the alpha-carbon cylinder, the mean inner diameter of the channel would be 2.8 nm and its mean outer diameter 4.8 nm. The former parameter is in excellent agreement with that inferred from negative stain exclusion, while the latter is consistent with the observed array spacings and X-ray scattering results (see above).

Estimates have been made of the number of 30-kDa polypeptides that form one VDAC channel based on space-filling considerations within the two-dimensional crystals (Mannella, 1985, 1987). For a constant inner channel diameter of 2.5 nm, the stoichiometry is either one or two polypeptides per channel, depending on whether lipids occupy 50% or 20% of the total unit cell volume, respectively. Three-dimensional reconstruction of unstained arrays will be needed to unambiguously distinguish between these two possibilities.

Channel Organization and Self-Assembly of the Arrays

While crystallization of the channels in the plane of the mitochondrial outer membrane is triggered by phospholipid removal, the distinctive array

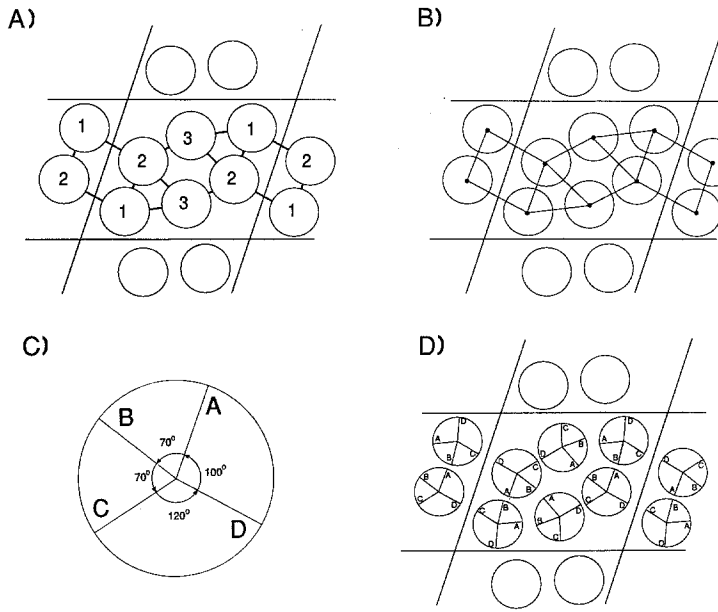

Fig. 2. Geometry of the interchannel contacts in the oblique VDAC array. (A) Channels are represented as projections of hollow cylinders (rings) with diameters of 3.8 nm. Channels whose positions are invariant with sliding are represented as linked or bonded. Note the two-fold rotational symmetry of the channel hexamer within the unit cell. Thus, although there are six channels in the unit cell, only three are not related by symmetry. (Any combination of channels 1, 2, 3 may be considered a crystallographic asymmetric unit.) (B) Simplified version of (A), showing the bonding angles with respect to the center of each channel. (C) Distribution of contact points on the channel periphery, inferred from the pattern of bonding in the array rows. (D) Array model generated using the single-channel model from (C).

geometries indicate that the process is not simply one of random close-packing. Ordering of the channels likely proceeds according to the basic principles which govern self-assembly processes (Caspar and Klug, 1962). To occur spontaneously, the ordered state must be energetically more favorable than that represented by random arrangement of proteins (and lipids). The source of the energy which drives the ordering is the formation of inter-subunit contacts or bonds. Thus, the arrangement of channels in the periodic VDAC array should reflect the pattern of bonds which the channels form with one another.

In Fig. 2A, an oblique VDAC array is shown schematically, with heavy dark bands used to indicate the invariant contacts between neighboring channels within horizontal rows. (Since the rows can slide with respect to each other, inter-row contacts are probably weak and so are not considered.) The pattern of the bonding between channels is indicated more clearly in Fig. 2B. There appears to be a common bonding pattern at each channel,

indicated by the model of Fig. 2C. This shows the channel as a projected cylinder that is divided into sectors by four radii (labeled A to D) with the indicated angular spacings. When the model is placed at each of the channel positions in the array and rotated appropriately (Fig. 2D), all the possible contacts are accounted for by only two types of bonds, namely A–B and C–D. Note that not each contact is a perfect match; some are offset a few degrees, which may relate to the slight variation in "bond lengths." (Center-to-center spacings between adjacent channels are 4.3–4.8 nm within the hexamer and 5.3 nm between adjacent hexamers).

Correlation of the Model with Previous Mapping Results

The above analysis suggests that the two-dimensional VDAC array may arise from self-assembly of identical rigid cylindrical subunits which can make only two types of contacts with each other. The "bonding model" in Fig. 2D predicts certain rotational orientations of the channels within the hexameric groups which make up the repeating unit of the array. For example, the C–D sectors of the cylinders are always turned to the outside of the channel hexamer while the A–B sectors tend to face inside the unit cell.

Figure 3 summarizes the results of electron microscopic mapping experiments with crystalline VDAC. In general, the results of these experiments support the bonding model derived above.

There are six probable phospholipid domains located around the outside of the channel hexamer (Fig. 3A) (Mannella *et al.*, 1986; Mannella, 1987; Mannella *et al.*, 1989). These are characterized as sites which stain lightly with uranyl (Ting-Beall, 1979) and which have low density in projections of unstained VDAC arrays. In terms of the model of Fig. 2D, the six phospholipid sites reduce to two classes: (i) Four sites are bounded by pairs of B–C and D–A sectors of four channels. (ii) The other two putative phospholipid domains are bounded only by C–D sectors of channels.

Cytochrome *c* is one of numerous polypeptides transported across the mitochondrial outer membrane after synthesis on cytoplasmic ribosomes (Neupert and Schatz, 1981). Addition of cytochrome *c* to VDAC arrays causes negative stain to be excluded from certain regions, which are thereby inferred to be sites of prominent binding of the protein to the array surface (Mannella *et al.*, 1987). These binding sites correspond to the class (ii) phospholipid domains (Fig. 3B). This apparent specificity of cytochrome *c* for a particular class of phospholipid domains is intriguing, especially since the domains are in contact with only one region of each VDAC channel, i.e., the C–D sectors. If the model of Fig. 2D is correct, the binding of

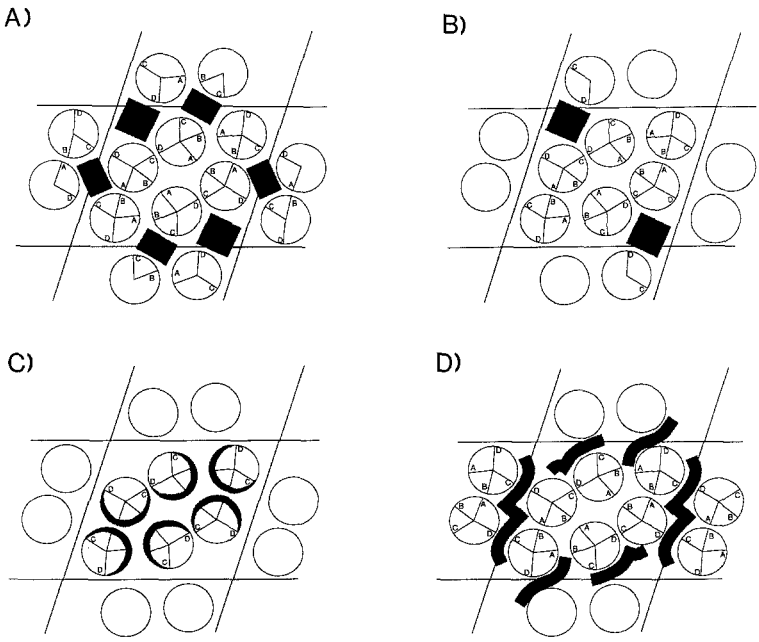

Fig. 3. Correlation between electron microscopic mapping results and the array model of Fig. 2D. Shaded regions correspond to (A) lipid domains, (B) cytochrome *c* binding sites, (C) clusters of accessible lysine residues, and (D) polyanionic modulator binding sites.

cytochrome *c* to the VDAC array may involve specific interaction of the cytochrome with the C–D sector of the channel.

The two-dimensional distribution of basic amino acids within the VDAC channel has been inferred from electron imaging experiments with succinylated arrays (Mannella and Frank, 1984, 1986). Phosphotungstate is an anionic stain with an affinity for positively charged amino acids (Tzaphlidou *et al.*, 1982). Its accumulation around the lumen of VDAC is reduced when the arrays are succinylated, a treatment which changes the charge at lysines from $+1$ to -1. [Succinylation also changes the ion selectivity of VDAC from anionic to cationic and abolishes voltage gating (Doring and Colombini, 1985), suggesting that some or all of the modified lysines are involved in both functional properties.] Regions of reduced phosphotungstate staining following succinylation have been inferred to correspond to areas with a high density of basic amino acids accessible to the aqueous medium. These regions were found to occur on the inside of the channel hexamer (Fig. 3C). According to the model of Fig. 2D, the C–D sectors are always turned to the outside of the hexamers. Thus, the C–D sector is predicted to have few exposed basic amino acids. This is consistent

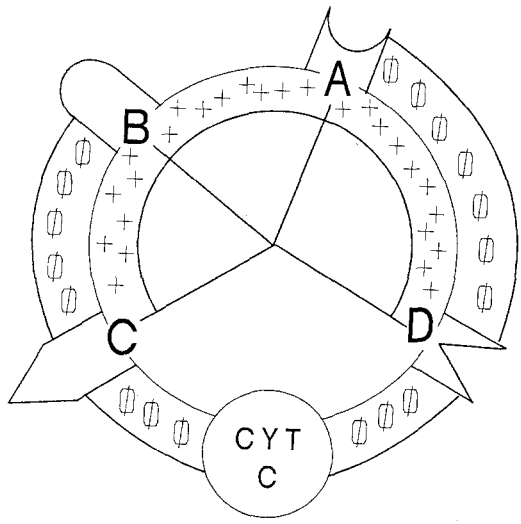

Fig. 4. Model summarizing the results of Figs. 2 and 3. The two pairs of bonding points are represented as complementary geometric shapes. The sectors whose inner surfaces are lysine-rich are indicated by +. The outer surfaces of sectors which contact lipid are indicated with ∅. The possible cytochrome *c* binding site in the C–D sector is also indicated.

with the preferred binding of cytochrome *c* (a basic polypeptide) to the vicinity of the C–D sector.

The sites of attachment of a synthetic polymer, known to alter the voltage-gating characteristics of VDAC (Colombini *et al.*, 1987; Benz *et al.*, 1988), have also been determined by negative-stain electron imaging experiments (Guo and Mannella, 1989, and submitted). The modulator, a copolymer of methacrylate, maleate, and styrene, was found to bind (i.e., exclude negative stain) predominantly along the outside of the channel hexamer (Fig. 3D). The amphiphilic nature of the polymer may account for its apparent affinity for these protein/lipid boundary regions. The polyanion appears to be excluded from the A–B sector of the channel, possibly related to the absence of channel–lipid contact in this region. Alternatively, the polyanion may be repelled by exposed acidic residues in this region.

Figure 4 summarizes the above electron microscopic mapping experiments in terms of the model of Fig. 2C. The channel is presumed to be a cylindrical beta-barrel, its axial projection divided radially into four sectors, demarcated by the four interchannel contacts, A through D. The cylindrical projection has an inner and an outer surface, composed of residues pointing inside and outside the cylinder, respectively. Three of the sectors, A–D, B–C, and C–D, make contact with lipid, suggesting that significant numbers of hydrophobic residues occur on the outer cylinder surface in these sectors.

Water-accessible basic amino acids occur along two-thirds of the projection, largely excluded from the C–D sector. These positively charged residues are present on the inner cylinder surface (the channel lumen) and/or at either edge of the cylinder (turn regions in the beta strands). There may be a specific site of interaction in the C–D sector with cytochrome *c*.

Acknowledgments

The contributions of the following to the research summarized in this report are gratefully acknowledged: Drs. J. Frank, M. Radermacher, and M. Colombini; also B. Cognon, X.-W. Guo, A. Ribeiro, and D. D'Arcangelis. This material is based upon work supported by grants PCM-8313045 and DMB-8613702 from the National Science Foundation.

References

Aquila, H., Link, T. A., and Klingenberg, M. (1987) *FEBS Lett.* **212**, 1–3.
Benz, R., Wojtczak, L., Bosch, W., and Brdiczka, D. (1988) *FEBS Lett.* **231**, 75–80.
Blachly-Dyson, E., Peng, S. Z., Colombini, M., and Forte, M. (1989) *J. Bioenerg. Biomembr.* **21**, 471–483.
Caspar, D. L. D., and Klug, A. (1962) *Cold Spring Harb. Symp. Quant. Biol.* **27**, 1–24.
Colombini, M. (1979) *Nature (London)* **279**, 643–645.
Colombini, M. (1983) *J. Membr. Biol.* **74**, 115–121.
Colombini, M., Yeung, C. L., Tung, J., and Konig, T. (1987) *Biochim. Biophys. Acta* **905**, 279–286.
Doring, C., and Colombini, M. (1985) *J. Membr. Biol.* **83**, 81–86.
Forte, M., Guy, R., and Mannella, C. A. (1987) *J. Bioenerg. Biomembr.* **19**, 341–350.
Freitag, H., Neupert, W., and Benz, R. (1982) *Eur. J. Biochem.* **123**, 629–639.
Guo, X.-W., and Mannella, C. A. (1989) *Biophys. J.* **55**, 211a.
Kleene, R., Pfanner, N., Pfaller, R., Link, T. A., Sebald, W., Neupert, W., and Tropschug, M. (1987) *EMBO J.* **6**, 2627–2633.
Linden, M., Gellerfors, P., and Nelson, B. D. (1982) *Biochem. J.* **208**, 77–82.
Mannella, C. A. (1982) *J. Cell Biol.* **94**, 680–687.
Mannella, C. A. (1984) *Science* **224**, 165–166.
Mannella, C. A. (1985) *Methods Enzymol.* **125**, 595–610.
Mannella, C. A. (1987) *J. Bioenerg. Biomembr.* **19**, 329–340.
Mannella, C. A. (1988) *J. Ultrastruct. Mol. Struct. Res.* **98**, 212–216.
Mannella, C. A. (1989) *Biochim. Biophys. Acta* **981**, 15–20.
Mannella, C. A., and Bonner, W. D., Jr. (1975) *Biochim. Biophys. Acta* **413**, 226–233.
Mannella, C. A., and Frank, J. (1984) *Ultramicroscopy* **13**, 93–102.
Mannella, C. A., and Auger, I. E. (1986) *Biophys. J.* **49**, 272a.
Mannella, C. A., and Frank, J. (1986) *J. Ultrastruct. Mol. Struct. Res.* **96**, 31–40.
Mannella, C. A., and Cognon, B. (1989) *Biophys. J.* **55**, 210a.
Mannella, C. A., Colombini, M., and Frank, J. (1983) *Proc. Natl. Acad. Sci. USA* **80**, 2243–2247.
Mannella, C. A., Radermacher, M., and Frank, J. (1984) In *Proceedings of the Electron Microscope Society of America* (Bailey, G. W., ed.), San Francisco Press, San Francisco, pp. 644–645.
Mannella, C. A., Ribeiro, A., and Frank, J. (1986) *Biophys. J.* **49**, 307–318.
Mannella, C. A., Ribeiro, A., and Frank, J. (1987) *Biophys. J.* **51**, 221–226.

Mannella, C. A., Guo, X.-W., and Cognon, B. (1989) *FEBS Lett.*, in press.
Mihara, K., and Sato, R. (1985) *EMBO J.* **4**, 769–774.
Neupert, W., and Schatz, G. (1981) *Trends Biochem. Sci.* **6** 1–4.
Parsons, D. P., Bonner, W. D., Jr., and Verboon, J. G. (1965). *Can. J. Bot.* **43**, 647–655.
Roos, N., Benz, R., and Brdiczka, D. (1982) *Biochim. Biophys. Acta* **686**, 204–214.
Schein, S. J., Colombini, M., and Finkelstein, A. (1976) *J. Membr. Biol.* **30**, 99–120.
Ting-Beall, H. P. (1979) *J. Microsc.* **118**, 221–227.
Tzaphlidou, M., Chapman, J. A., and Meek, K. M. (1982) *Micron* **13**, 119–131.
Young, S. H., and Poo, M. (1983) *Nature* **304**, 161–163.
Zalman, L. S., Nikaido, H., and Kagawa, Y. (1980) *J. Biol. Chem.* **255**, 1771–1774.